SIMULATING AMBIT PROCESSES USING THE HYBRID SCHEME

Mikko Pakkanen[1,2]

[1]Department of Mathematics, Imperial College London, UK
[2]CREATES, Aarhus University, Denmark

Conference on Ambit Fields and Related Topics
Aarhus, 17 August 2016

Joint work with Mikkel Bennedsen, Claudio Heinrich, Asger Lunde, and Almut Veraart

Imperial College London

CREATES
Center for Research in Econometric Analysis of Time Series

Introduction

Hybrid scheme for $\mathcal{BSS}$ processes

Hybrid scheme for 2-parameter $\mathcal{VMMA}$ fields

Simulating ambit processes and fields

We are interested in developing efficient simulation methods for ambit processes and fields of the form

$$X(\boldsymbol{t}) := \int_{\mathbb{R}^d} g(\boldsymbol{t}-\boldsymbol{s})\sigma(\boldsymbol{s})W(\mathrm{d}\boldsymbol{s}), \quad \boldsymbol{t} \in \mathbb{R}^d,$$

where W is a Gaussian white noise on $\mathbb{R}^d$.

Simulating ambit processes and fields

We are interested in developing efficient simulation methods for ambit processes and fields of the form

$$X(\boldsymbol{t}) := \int_{\mathbb{R}^d} g(\boldsymbol{t}-\boldsymbol{s})\sigma(\boldsymbol{s})W(\mathrm{d}\boldsymbol{s}), \quad \boldsymbol{t} \in \mathbb{R}^d,$$

where W is a Gaussian white noise on $\mathbb{R}^d$.

Power-law kernel functions

- We concentrate on the case where the kernel function g exhibits (possibly explosive) power-law behaviour near $\mathbf{0}$.

Simulating ambit processes and fields

We are interested in developing efficient simulation methods for ambit processes and fields of the form

$$X(\boldsymbol{t}) := \int_{\mathbb{R}^d} g(\boldsymbol{t}-\boldsymbol{s})\sigma(\boldsymbol{s})W(\mathrm{d}\boldsymbol{s}), \quad \boldsymbol{t} \in \mathbb{R}^d,$$

where W is a Gaussian white noise on $\mathbb{R}^d$.

Power-law kernel functions

- We concentrate on the case where the kernel function g exhibits (possibly explosive) power-law behaviour near $\mathbf{0}$.
- Such kernel functions give rise to ambit fields X, whose realisations are rougher or smoother, in terms of Hölder regularity, than those of a Brownian motion/sheet.

The Gaussian case

If the volatility field σ is constant and non-random, then X is stationary and (centred) Gaussian with covariance

$$\gamma(\boldsymbol{h}) := \mathbb{E}\big(X(\mathbf{0})X(\boldsymbol{h})\big) = \int_{\mathbb{R}^d} g(\boldsymbol{h}+\boldsymbol{x})g(\boldsymbol{x})\mathrm{d}\boldsymbol{x}, \quad \boldsymbol{h} \in \mathbb{R}^d.$$

The Gaussian case

If the volatility field σ is constant and non-random, then X is stationary and (centred) Gaussian with covariance

$$\gamma(\boldsymbol{h}) := \mathbb{E}\big(X(\mathbf{0})X(\boldsymbol{h})\big) = \int_{\mathbb{R}^d} g(\boldsymbol{h}+\boldsymbol{x})g(\boldsymbol{x})\mathrm{d}\boldsymbol{x}, \quad \boldsymbol{h} \in \mathbb{R}^d.$$

Now X can be simulated exactly by sampling from a multivariate Gaussian distribution, determined by γ.

The Gaussian case

If the volatility field σ is constant and non-random, then X is stationary and (centred) Gaussian with covariance

$$\gamma(\boldsymbol{h}) := \mathbb{E}\big(X(\boldsymbol{0})X(\boldsymbol{h})\big) = \int_{\mathbb{R}^d} g(\boldsymbol{h}+\boldsymbol{x})g(\boldsymbol{x})\mathrm{d}\boldsymbol{x}, \quad \boldsymbol{h} \in \mathbb{R}^d.$$

Now X can be simulated exactly by sampling from a multivariate Gaussian distribution, determined by γ.

Caveats of exact Gaussian simulation

- It can be computationally costly, but efficient implementations using circulant matrices are available (Wood and Chan, 1994).

The Gaussian case

If the volatility field σ is constant and non-random, then X is stationary and (centred) Gaussian with covariance

$$\gamma(\boldsymbol{h}) := \mathbb{E}\big(X(\boldsymbol{0})X(\boldsymbol{h})\big) = \int_{\mathbb{R}^d} g(\boldsymbol{h}+\boldsymbol{x})g(\boldsymbol{x})\mathrm{d}\boldsymbol{x}, \quad \boldsymbol{h} \in \mathbb{R}^d.$$

Now X can be simulated exactly by sampling from a multivariate Gaussian distribution, determined by γ.

Caveats of exact Gaussian simulation

- It can be computationally costly, but efficient implementations using circulant matrices are available (Wood and Chan, 1994).
- The covariance γ is sometimes difficult evaluate numerically.

The Gaussian case

If the volatility field σ is constant and non-random, then X is stationary and (centred) Gaussian with covariance

$$\gamma(\boldsymbol{h}) := \mathbb{E}\big(X(\boldsymbol{0})X(\boldsymbol{h})\big) = \int_{\mathbb{R}^d} g(\boldsymbol{h}+\boldsymbol{x})g(\boldsymbol{x})\mathrm{d}\boldsymbol{x}, \quad \boldsymbol{h} \in \mathbb{R}^d.$$

Now X can be simulated exactly by sampling from a multivariate Gaussian distribution, determined by γ.

Caveats of exact Gaussian simulation

- It can be computationally costly, but efficient implementations using circulant matrices are available (Wood and Chan, 1994).
- The covariance γ is sometimes difficult evaluate numerically.
- The approach does not extend to the case where σ is stochastic.

Approximation by Riemann sums

In general, exactness of simulation is a tall order, and we instead try to approximate X — hopefully precisely enough.

Approximation by Riemann sums

In general, exactness of simulation is a tall order, and we instead try to approximate X — hopefully precisely enough.

Riemann sum approximation of X

- We choose disjoint discretisation cells $C_1, C_2, \ldots \subset \mathbb{R}^d$ such that $\mathbb{R}^d = \bigcup_{i=1}^{\infty} C_i$, and fix $\boldsymbol{c}_i \in C_i$ for each $i \in \mathbb{N}$.

Approximation by Riemann sums

In general, exactness of simulation is a tall order, and we instead try to approximate X — hopefully precisely enough.

Riemann sum approximation of X

- We choose disjoint discretisation cells $C_1, C_2, \ldots \subset \mathbb{R}^d$ such that $\mathbb{R}^d = \bigcup_{i=1}^{\infty} C_i$, and fix $\boldsymbol{c}_i \in C_i$ for each $i \in \mathbb{N}$.
- We then approximate

$$X(\boldsymbol{t}) = \sum_{i=1}^{\infty} \int_{C_i} g(\boldsymbol{t}-\boldsymbol{s})\sigma(\boldsymbol{s})W(\mathrm{d}\boldsymbol{s}) \approx \sum_{i=1}^{N} g(\boldsymbol{t}-\boldsymbol{c}_i)\sigma(\boldsymbol{c}_i)W(C_i),$$

where N is such that $C_1, \ldots, C_N$ provide "enough" coverage.

Poor precision of Riemann sums

In particular, this approach amounts to approximating the kernel function g by a piecewise constant function.

Poor precision of Riemann sums

In particular, this approach amounts to approximating the kernel function g by a piecewise constant function.

When g has power-law behaviour near $\mathbf{0}$, the approximation

$$g(\boldsymbol{t}-\boldsymbol{s}) \approx g(\boldsymbol{t}-\boldsymbol{c}_i), \quad \boldsymbol{s} \in C_i,$$

can be very poor for any cell C_i such that $\boldsymbol{c}_i \approx \boldsymbol{t}$, as g is evaluated near $\mathbf{0}$ therein.

Poor precision of Riemann sums

In particular, this approach amounts to approximating the kernel function g by a piecewise constant function.

When g has power-law behaviour near $\mathbf{0}$, the approximation

$$g(\boldsymbol{t}-\boldsymbol{s}) \approx g(\boldsymbol{t}-\boldsymbol{c}_i), \quad \boldsymbol{s} \in C_i,$$

can be very poor for any cell C_i such that $\boldsymbol{c}_i \approx \boldsymbol{t}$, as g is evaluated near $\mathbf{0}$ therein.

The resulting Riemann sum approximation of X will be poor as well.

Poor precision of Riemann sums

In particular, this approach amounts to approximating the kernel function g by a piecewise constant function.

When g has power-law behaviour near $\mathbf{0}$, the approximation

$$g(\boldsymbol{t}-\boldsymbol{s}) \approx g(\boldsymbol{t}-\boldsymbol{c}_i), \quad \boldsymbol{s} \in C_i,$$

can be very poor for any cell C_i such that $\boldsymbol{c}_i \approx \boldsymbol{t}$, as g is evaluated near $\mathbf{0}$ therein.

The resulting Riemann sum approximation of X will be poor as well.

Solution

The hybrid scheme solves this problem by using a more appropriate "bespoke" approximation of g near $\mathbf{0}$.

Introduction

Hybrid scheme for $\mathcal{BSS}$ processes

Hybrid scheme for 2-parameter $\mathcal{VMMA}$ fields

Brownian semistationary processes

Definition (Barndorff-Nielsen and Schmiegel, 2009)

Let $(\Omega, \mathscr{F}, \{\mathscr{F}_t\}_{t\in\mathbb{R}}, \mathbf{P})$ be a filtered probability space supporting a Brownian motion $\{W(t)\}_{t\in\mathbb{R}}$.

Brownian semistationary processes

Definition (Barndorff-Nielsen and Schmiegel, 2009)

Let $(\Omega, \mathscr{F}, \{\mathscr{F}_t\}_{t\in\mathbb{R}}, \mathbf{P})$ be a filtered probability space supporting a Brownian motion $\{W(t)\}_{t\in\mathbb{R}}$.

A Brownian semistationary ($\mathcal{BSS}$) process $\{X(t)\}_{t\in\mathbb{R}}$ is defined by

$$X(t) := \int_{-\infty}^{t} g(t-s)\sigma(s)\mathrm{d}W(s),$$

where

- $g : (0,\infty) \to [0,\infty)$ is a square-integrable function,
- $\{\sigma(t)\}_{t\in\mathbb{R}}$ is an adapted covariance-stationary process with locally bounded trajectories.

Standing assumptions

We first give a precise description of power-law behaviour near 0:

Standing assumptions

We first give a precise description of power-law behaviour near 0:

Assumption

I For some $\alpha \in \left(-\frac{1}{2}, \frac{1}{2}\right) \setminus \{0\}$,

$$g(x) = x^{\alpha} L_g(x), \quad x \in (0,1],$$

where $L_g : (0,1] \to [0,\infty)$ is C^1, slowly varying at 0 Definition and bounded away from 0.

Standing assumptions

We first give a precise description of power-law behaviour near 0:

Assumption

- For some $\alpha \in \left(-\frac{1}{2}, \frac{1}{2}\right) \setminus \{0\}$,

$$g(x) = x^{\alpha} L_g(x), \quad x \in (0,1],$$

where $L_g : (0,1] \to [0,\infty)$ is C^1, slowly varying at 0 ▸ Definition and bounded away from 0. Moreover, there exists a constant $C > 0$ such that the derivative L_g' of L_g satisfies

$$|L_g'(x)| \leq C(1 + x^{-1}), \quad x \in (0,1].$$

Standing assumptions

The remaining assumptions serve a more technical purpose:

Assumption

II The function g is C^1 on $(0,\infty)$, so that its derivative g' is ultimately monotonic and satisfies $\int_1^\infty g'(x)^2 dx < \infty$.

Standing assumptions

The remaining assumptions serve a more technical purpose:

Assumption

II The function g is C^1 on $(0,\infty)$, so that its derivative g' is ultimately monotonic and satisfies $\int_1^\infty g'(x)^2 dx < \infty$.

III For some $\beta \in \left(-\infty, -\frac{1}{2}\right)$, we have $g(x) = \mathcal{O}(x^\beta)$, $x \to \infty$.

Standing assumptions

The remaining assumptions serve a more technical purpose:

Assumption

II The function g is C^1 on $(0,\infty)$, so that its derivative g' is ultimately monotonic and satisfies $\int_1^\infty g'(x)^2 dx < \infty$.

III For some $\beta \in \left(-\infty, -\frac{1}{2}\right)$, we have $g(x) = \mathcal{O}(x^\beta)$, $x \to \infty$.

Example

The so-called gamma kernel

$$g(x) = x^\alpha e^{-\lambda x}, \quad x \in (0,\infty),$$

for any $\alpha \in \left(-\frac{1}{2}, \frac{1}{2}\right) \setminus \{0\}$ and $\lambda > 0$ satisfies these assumptions.

Remark about stationarity and regularity

Proposition (Bennedsen, Lunde, P., 2015)

1. *The process X is centred and covariance stationary.*
2. *For any $t \in \mathbb{R}$,*

$$\mathbb{E}\left(|X(s)-X(t)|^2\right) \sim \mathbb{E}\left(\sigma(0)^2\right) C_\alpha |s-t|^{2\alpha+1} L_g(|s-t|)^2$$

   as $s \to t$, where $C_\alpha = \frac{1}{2\alpha+1} + \int_0^\infty \left((y+1)^\alpha - y^\alpha\right)^2 dy$.
3. *The process X has a modification with locally ϕ-Hölder continuous trajectories for any $\phi \in \left(0, \alpha + \frac{1}{2}\right)$.*

Remark about stationarity and regularity

Proposition (Bennedsen, Lunde, P., 2015)

1. *The process X is centred and covariance stationary.*
2. *For any $t \in \mathbb{R}$,*

$$\mathbb{E}\left(|X(s) - X(t)|^2\right) \sim \mathbb{E}\left(\sigma(0)^2\right) C_\alpha |s-t|^{2\alpha+1} L_g(|s-t|)^2$$

as $s \to t$, where $C_\alpha = \frac{1}{2\alpha+1} + \int_0^\infty \left((y+1)^\alpha - y^\alpha\right)^2 dy$.

3. *The process X has a modification with locally ϕ-Hölder continuous trajectories for any $\phi \in \left(0, \alpha + \frac{1}{2}\right)$.*

Definition

We refer to α as the roughness parameter of X.

Approximation by Riemann sums

In the $\mathcal{BSS}$ case, the conventional approximation of $X(t)$ by Riemann sums can be expressed as

$$
\begin{aligned}
X(t) &= \sum_{k=1}^{\infty} \int_{t-\frac{k}{n}}^{t-\frac{k}{n}+\frac{1}{n}} g(t-s)\sigma(s)\,\mathrm{d}W(s) \\
&\approx \sum_{k=1}^{N_n} g\left(\frac{k}{n}\right)\sigma\left(t-\frac{k}{n}\right)\left(W\left(t-\frac{k}{n}+\frac{1}{n}\right)-W\left(t-\frac{k}{n}\right)\right),
\end{aligned}
$$

where $N_n \to \infty$ as $n \to \infty$.

Approximation by Riemann sums

In the $\mathcal{BSS}$ case, the conventional approximation of $X(t)$ by Riemann sums can be expressed as

$$X(t) = \sum_{k=1}^{\infty} \int_{t-\frac{k}{n}}^{t-\frac{k}{n}+\frac{1}{n}} g(t-s)\sigma(s)\mathrm{d}W(s)$$
$$\approx \sum_{k=1}^{N_n} g\Big(\frac{k}{n}\Big)\sigma\Big(t-\frac{k}{n}\Big)\Big(W\Big(t-\frac{k}{n}+\frac{1}{n}\Big)-W\Big(t-\frac{k}{n}\Big)\Big),$$

where $N_n \to \infty$ as $n \to \infty$.

- As mentioned before, this corresponds to approximating g by a step function.
- The scheme can be very inaccurate when g is singular, $\alpha < 0$.
- The first summands are the problematic ones, as g is evaluated near zero therein.

Approximation by Riemann sums

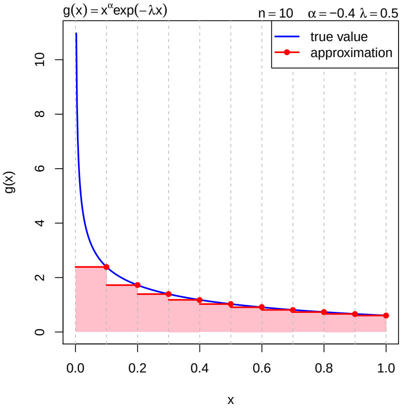

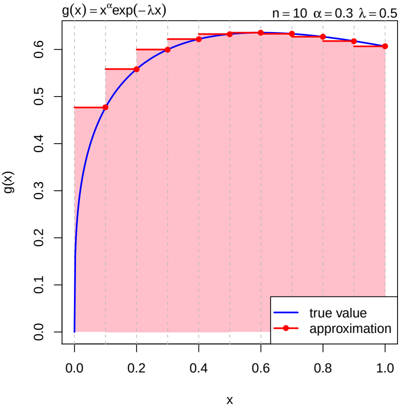

Hybrid scheme for $\mathcal{BSS}$ processes

The idea behind the hybrid scheme (Bennedsen, Lunde, P., 2015) is to replace the first $\kappa \geqslant 1$ Riemann summands by suitable random variables that provide a better approximation.

Hybrid scheme for $\mathcal{BSS}$ processes

The idea behind the hybrid scheme (Bennedsen, Lunde, P., 2015) is to replace the first $\kappa \geqslant 1$ Riemann summands by suitable random variables that provide a better approximation.

We use for $k = 1, \ldots, \kappa$,

$$g(t-s) \approx (t-s)^{\alpha} L_g\Big(\frac{k}{n}\Big), \quad t-s \in \Big[\frac{k-1}{n}, \frac{k}{n}\Big] \setminus \{0\},$$

motivated by the properties slowly varying functions, and define

$$\check{X}_n(t) := \sum_{k=1}^{\kappa} L_g\Big(\frac{k}{n}\Big) \sigma\Big(t - \frac{k}{n}\Big) \int_{t-\frac{k}{n}}^{t-\frac{k}{n}+\frac{1}{n}} (t-s)^{\alpha} dW(s).$$

Hybrid scheme for $\mathcal{BSS}$ processes

We retain Riemann summands for the remaining discretisation cells, but we allow the point at which g is evaluated to be choosen freely within each cell.

Hybrid scheme for $\mathcal{BSS}$ processes

We retain Riemann summands for the remaining discretisation cells, but we allow the point at which g is evaluated to be choosen freely within each cell.

We define

$$\hat{X}_n(t) := \sum_{k=\kappa+1}^{N_n} g\left(\frac{b_k}{n}\right)\sigma\left(t-\frac{k}{n}\right)\left(W\left(t-\frac{k}{n}+\frac{1}{n}\right)-W\left(t-\frac{k}{n}\right)\right),$$

where $\mathbf{b} = \{b_k\}_{k=\kappa+1}^{\infty}$ is a sequence that must satisfy

$$b_k \in [k-1, k] \setminus \{0\}, \quad k \geqslant \kappa+1,$$

but otherwise can be chosen freely.

Hybrid scheme for $\mathcal{BSS}$ processes

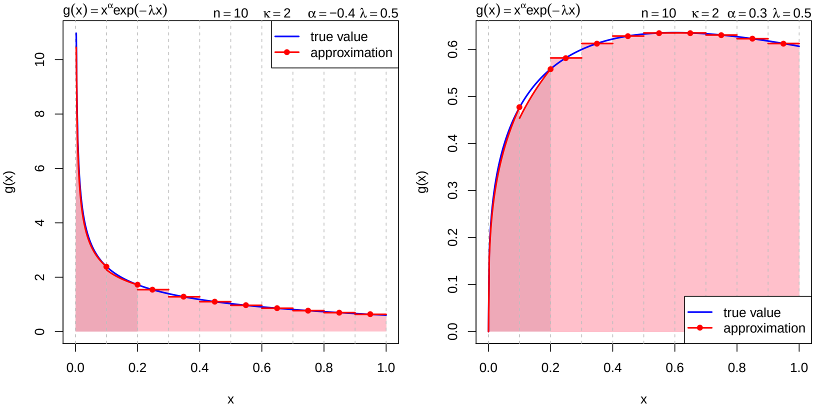

Hybrid scheme for $\mathcal{BSS}$ processes

The hybrid scheme for $X(t)$ is then given by

$$X(t) \approx X_n(t) := \check{X}_n(t) + \hat{X}_n(t).$$

Remark

Define $\mathbf{b}_0 := \{k\}_{k=\kappa+1}^{\infty}$. Then in the case $\kappa = 0$ and $\mathbf{b} = \mathbf{b}_0$ we recover the approximation by Riemann sums.

Hybrid scheme for $\mathcal{BSS}$ processes

The hybrid scheme for $X(t)$ is then given by

$$X(t) \approx X_n(t) := \check{X}_n(t) + \hat{X}_n(t).$$

Remark

Define $\mathbf{b}_0 := \{k\}_{k=\kappa+1}^{\infty}$. Then in the case $\kappa = 0$ and $\mathbf{b} = \mathbf{b}_0$ we recover the approximation by Riemann sums.

Assumption

IV We have $N_n \sim n^{\gamma+1}$ as $n \to \infty$ for some $\gamma > 0$.

▸ Implementation

Asymptotics of the mean square error

Theorem (Bennedsen, Lunde, P., 2015)

Suppose that $\gamma > -\frac{2\alpha+1}{2\beta+1}$ *and that for some* $\delta > 0$,

$$\mathbb{E}\left(|\sigma(s) - \sigma(0)|^2\right) = \mathcal{O}\left(s^{2\alpha+1+\delta}\right), \quad s \to 0+.$$

Asymptotics of the mean square error

Theorem (Bennedsen, Lunde, P., 2015)

Suppose that $\gamma > -\frac{2\alpha+1}{2\beta+1}$ *and that for some* $\delta > 0$*,*

$$\mathbb{E}\left(|\sigma(s)-\sigma(0)|^2\right) = \mathcal{O}\left(s^{2\alpha+1+\delta}\right), \quad s \to 0+.$$

Then for all $t \in \mathbb{R}$*,*

$$\mathbb{E}\left(|X(t)-X_n(t)|^2\right) \sim J(\alpha,\kappa,\mathbf{b})\mathbb{E}\left(\sigma(0)^2\right) n^{-(2\alpha+1)} L_g(1/n)^2, \quad n \to \infty,$$

where

$$J(\alpha,\kappa,\mathbf{b}) := \sum_{k=\kappa+1}^{\infty} \int_{k-1}^{k} (y^\alpha - b_k^\alpha)^2 dy < \infty.$$

Asymptotic root mean square error

The quantity $\sqrt{J(\alpha,\kappa,\mathbf{b})}$ can be seen as the asymptotic RMSE of the hybrid scheme.

Asymptotic root mean square error

The quantity $\sqrt{J(\alpha,\kappa,\mathbf{b})}$ can be seen as the asymptotic RMSE of the hybrid scheme.

For any $\alpha \in \left(-\frac{1}{2}, \frac{1}{2}\right) \setminus \{0\}$, we can find $\mathbf{b}$ that minimises $\sqrt{J(\alpha,\kappa,\mathbf{b})}$. We denote the minimiser by $\mathbf{b}^*$.

Asymptotic root mean square error

The quantity $\sqrt{J(\alpha,\kappa,\mathbf{b})}$ can be seen as the asymptotic RMSE of the hybrid scheme.

For any $\alpha \in \left(-\frac{1}{2},\frac{1}{2}\right) \setminus \{0\}$, we can find $\mathbf{b}$ that minimises $\sqrt{J(\alpha,\kappa,\mathbf{b})}$. We denote the minimiser by $\mathbf{b}^*$.

It is illuminating to assess the asymptotic improvement on the approximation by Riemann sums:

$$\text{reduction in asymptotic RMSE} = \frac{\sqrt{J(\alpha,\kappa,\mathbf{b})}-\sqrt{J(\alpha,0,\mathbf{b}_0)}}{\sqrt{J(\alpha,0,\mathbf{b}_0)}} \cdot 100\%.$$

Asymptotic root mean square error

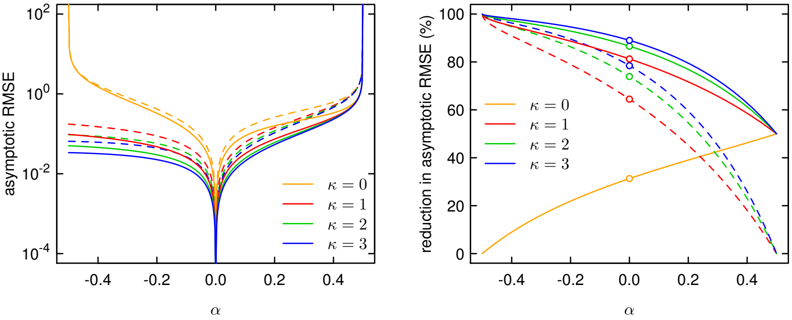

Solid line: $\mathbf{b} = \mathbf{b}^*$; dashed line: $\mathbf{b} = \mathbf{b}_0$.

Simulated trajectories

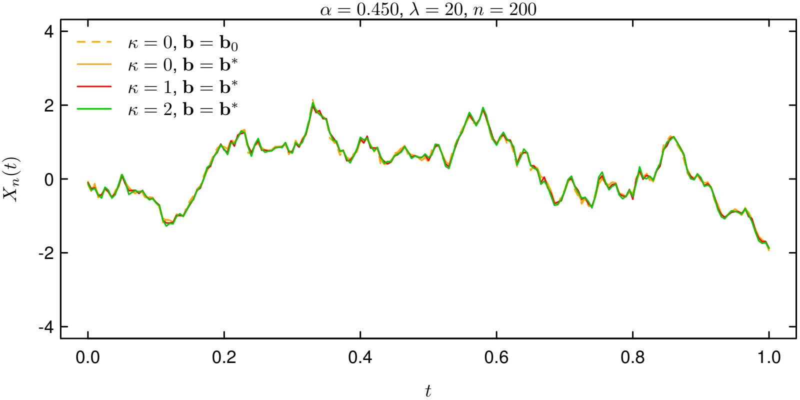

Using $g(x) = c_{\alpha,\lambda} x^{\alpha} e^{-\lambda x}$, with $c_{\alpha,\lambda}$ such that $\int_0^{\infty} g(x)^2 \mathrm{d}x = 1$.

Simulated trajectories

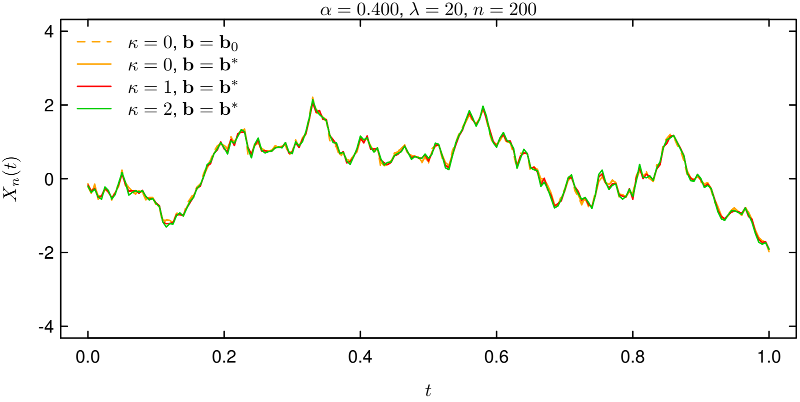

Using $g(x) = c_{\alpha,\lambda} x^{\alpha} e^{-\lambda x}$, with $c_{\alpha,\lambda}$ such that $\int_0^{\infty} g(x)^2 \mathrm{d}x = 1$.

Simulated trajectories

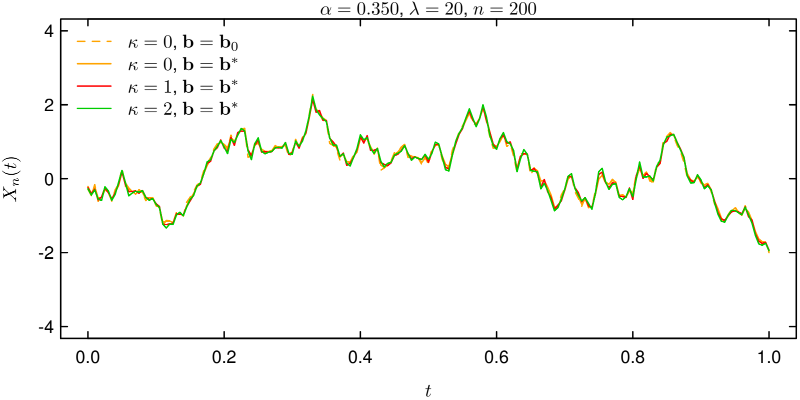

Using $g(x) = c_{\alpha,\lambda} x^{\alpha} e^{-\lambda x}$, with $c_{\alpha,\lambda}$ such that $\int_0^\infty g(x)^2 \mathrm{d}x = 1$.

Simulated trajectories

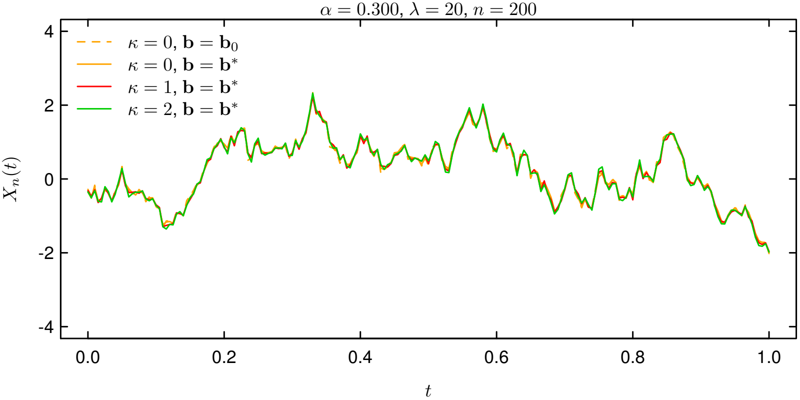

Using $g(x) = c_{\alpha,\lambda} x^{\alpha} e^{-\lambda x}$, with $c_{\alpha,\lambda}$ such that $\int_0^{\infty} g(x)^2 \mathrm{d}x = 1$.

Simulated trajectories

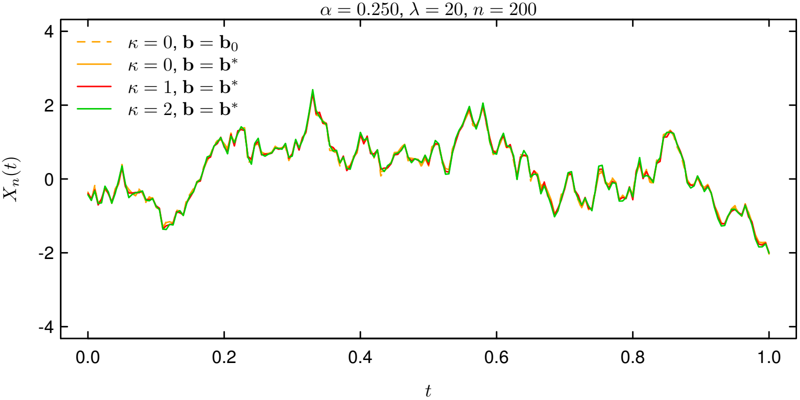

Using $g(x) = c_{\alpha,\lambda} x^{\alpha} e^{-\lambda x}$, with $c_{\alpha,\lambda}$ such that $\int_0^\infty g(x)^2 \mathrm{d}x = 1$.

Simulated trajectories

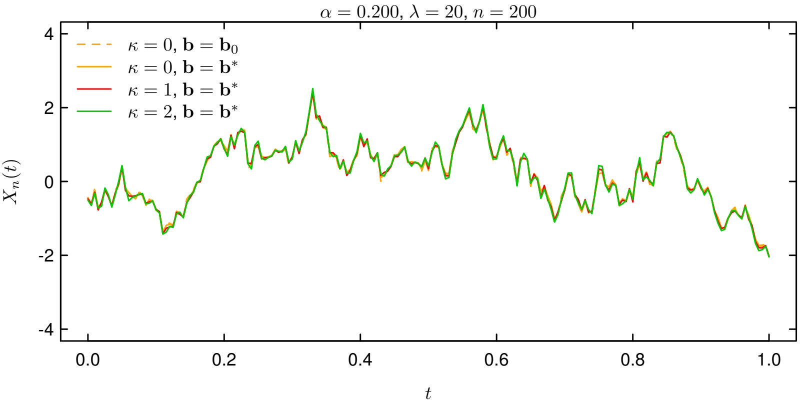

Using $g(x) = c_{\alpha,\lambda} x^{\alpha} e^{-\lambda x}$, with $c_{\alpha,\lambda}$ such that $\int_0^{\infty} g(x)^2 \mathrm{d}x = 1$.

Simulated trajectories

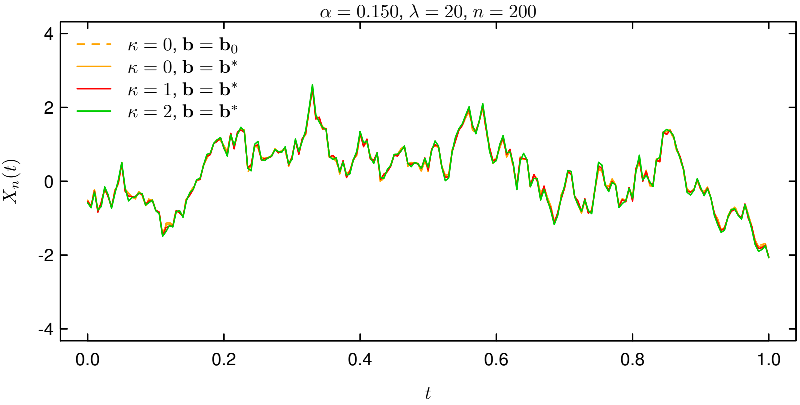

Using $g(x) = c_{\alpha,\lambda} x^{\alpha} e^{-\lambda x}$, with $c_{\alpha,\lambda}$ such that $\int_0^{\infty} g(x)^2 \mathrm{d}x = 1$.

Simulated trajectories

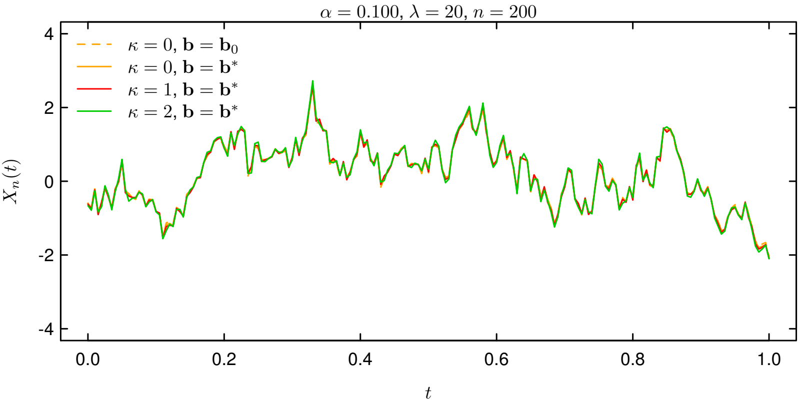

Using $g(x) = c_{\alpha,\lambda} x^{\alpha} e^{-\lambda x}$, with $c_{\alpha,\lambda}$ such that $\int_0^{\infty} g(x)^2 \mathrm{d}x = 1$.

Simulated trajectories

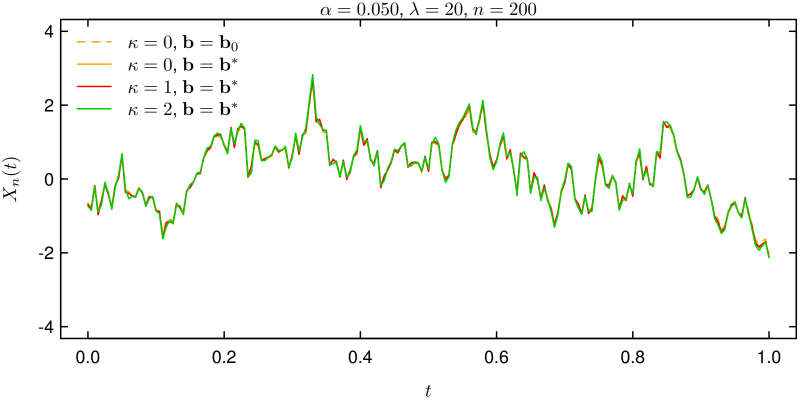

Using $g(x) = c_{\alpha,\lambda} x^{\alpha} e^{-\lambda x}$, with $c_{\alpha,\lambda}$ such that $\int_0^\infty g(x)^2 \mathrm{d}x = 1$.

Simulated trajectories

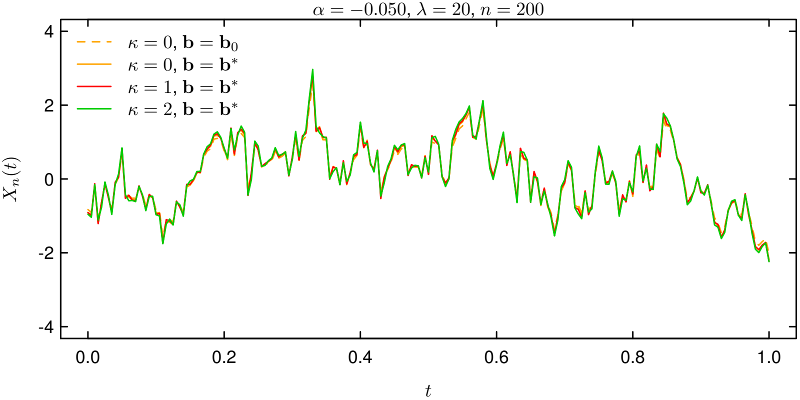

Using $g(x) = c_{\alpha,\lambda} x^{\alpha} e^{-\lambda x}$, with $c_{\alpha,\lambda}$ such that $\int_0^\infty g(x)^2 \mathrm{d}x = 1$.

Simulated trajectories

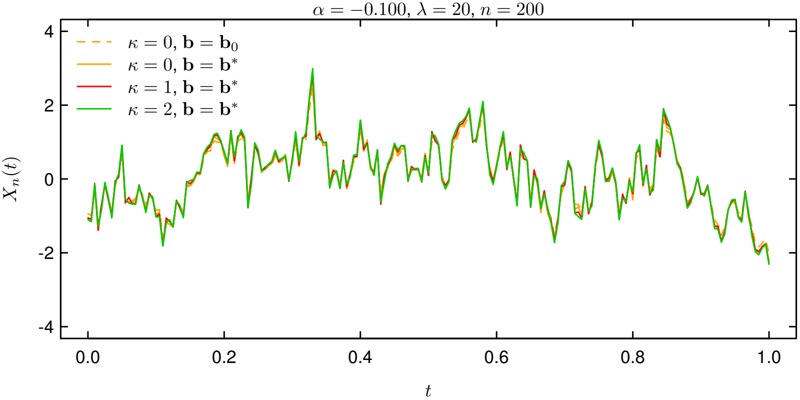

Using $g(x) = c_{\alpha,\lambda} x^{\alpha} e^{-\lambda x}$, with $c_{\alpha,\lambda}$ such that $\int_0^{\infty} g(x)^2 \mathrm{d}x = 1$.

Simulated trajectories

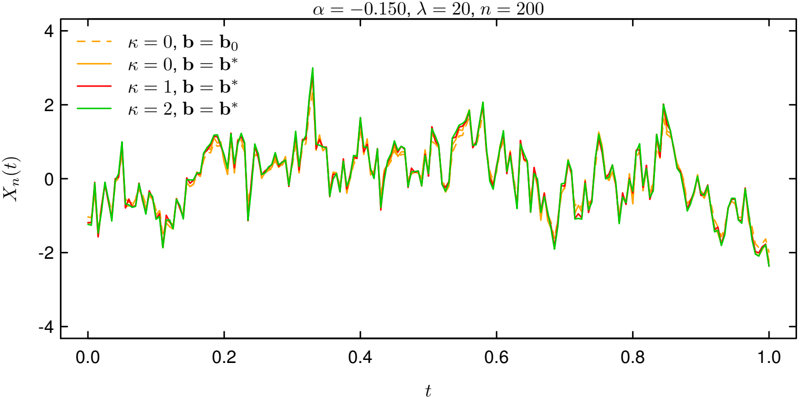

Using $g(x) = c_{\alpha,\lambda} x^{\alpha} e^{-\lambda x}$, with $c_{\alpha,\lambda}$ such that $\int_0^\infty g(x)^2 \mathrm{d}x = 1$.

Simulated trajectories

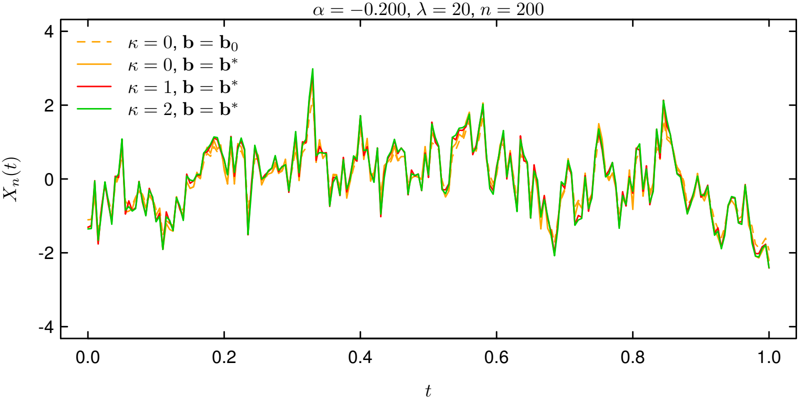

Using $g(x) = c_{\alpha,\lambda} x^{\alpha} e^{-\lambda x}$, with $c_{\alpha,\lambda}$ such that $\int_0^{\infty} g(x)^2 \mathrm{d}x = 1$.

Simulated trajectories

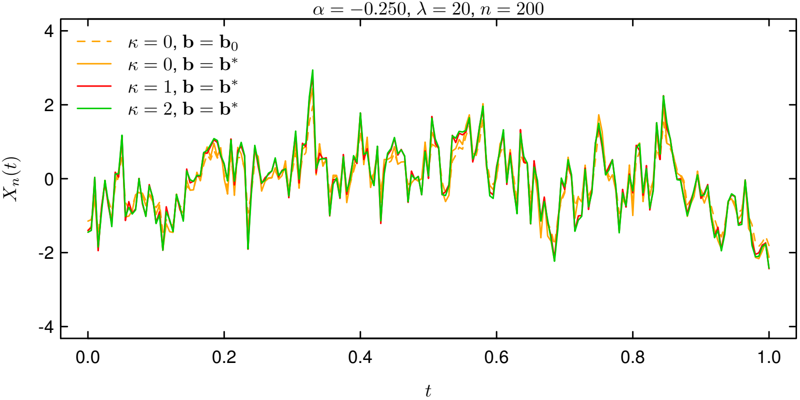

Using $g(x) = c_{\alpha,\lambda} x^{\alpha} e^{-\lambda x}$, with $c_{\alpha,\lambda}$ such that $\int_0^{\infty} g(x)^2 \mathrm{d}x = 1$.

Simulated trajectories

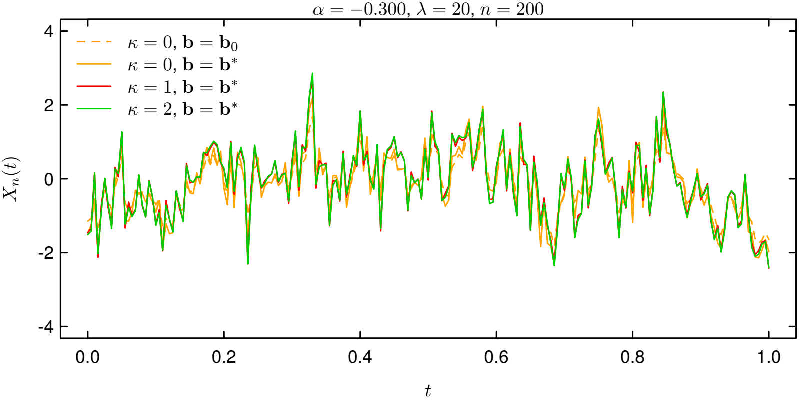

Using $g(x) = c_{\alpha,\lambda} x^{\alpha} e^{-\lambda x}$, with $c_{\alpha,\lambda}$ such that $\int_0^{\infty} g(x)^2 \mathrm{d}x = 1$.

Simulated trajectories

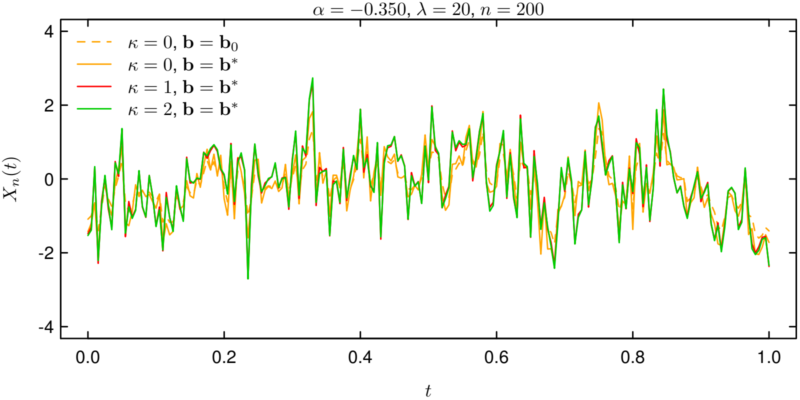

Using $g(x) = c_{\alpha,\lambda} x^{\alpha} e^{-\lambda x}$, with $c_{\alpha,\lambda}$ such that $\int_0^{\infty} g(x)^2 \mathrm{d}x = 1$.

Simulated trajectories

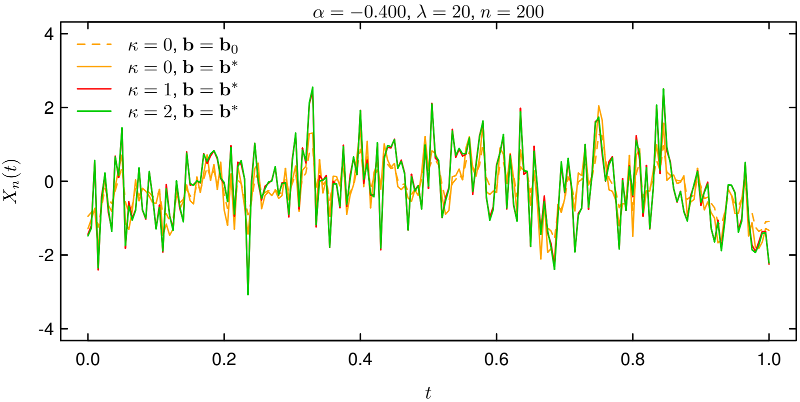

Using $g(x) = c_{\alpha,\lambda} x^{\alpha} e^{-\lambda x}$, with $c_{\alpha,\lambda}$ such that $\int_0^\infty g(x)^2 \mathrm{d}x = 1$.

Simulated trajectories

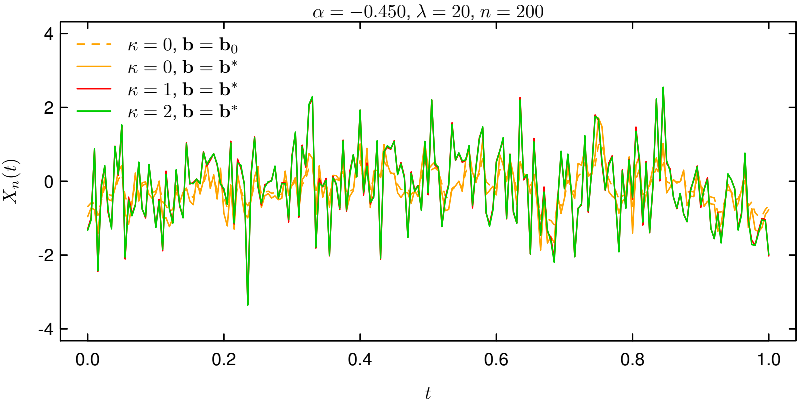

Using $g(x) = c_{\alpha,\lambda} x^{\alpha} e^{-\lambda x}$, with $c_{\alpha,\lambda}$ such that $\int_0^\infty g(x)^2 \mathrm{d}x = 1$.

Simulated trajectories

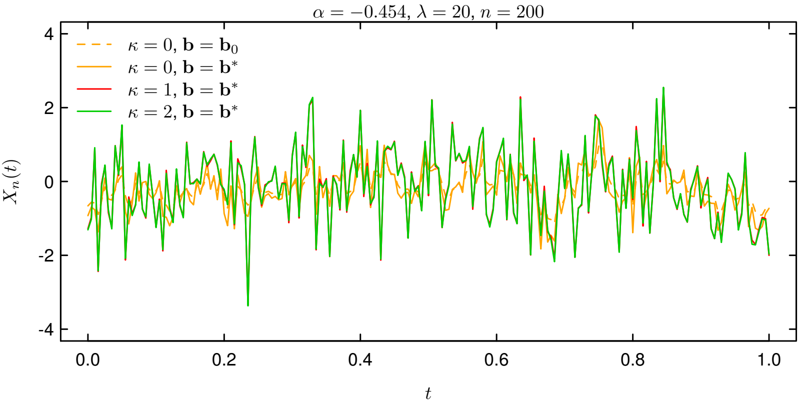

Using $g(x) = c_{\alpha,\lambda} x^{\alpha} e^{-\lambda x}$, with $c_{\alpha,\lambda}$ such that $\int_0^\infty g(x)^2 \mathrm{d}x = 1$.

Simulated trajectories

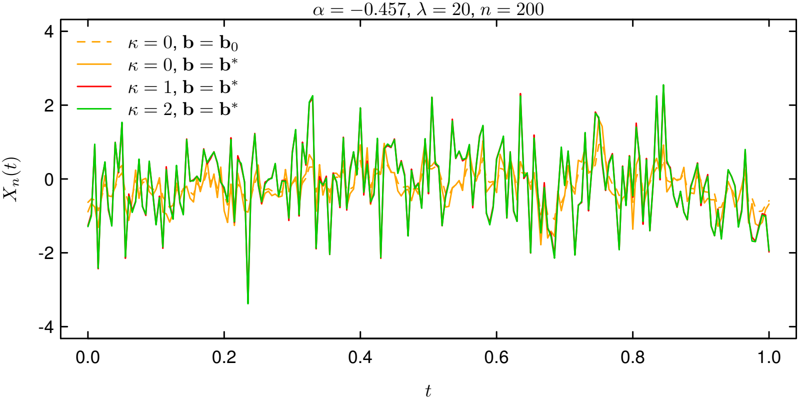

Using $g(x) = c_{\alpha,\lambda} x^{\alpha} e^{-\lambda x}$, with $c_{\alpha,\lambda}$ such that $\int_0^\infty g(x)^2 \mathrm{d}x = 1$.

Simulated trajectories

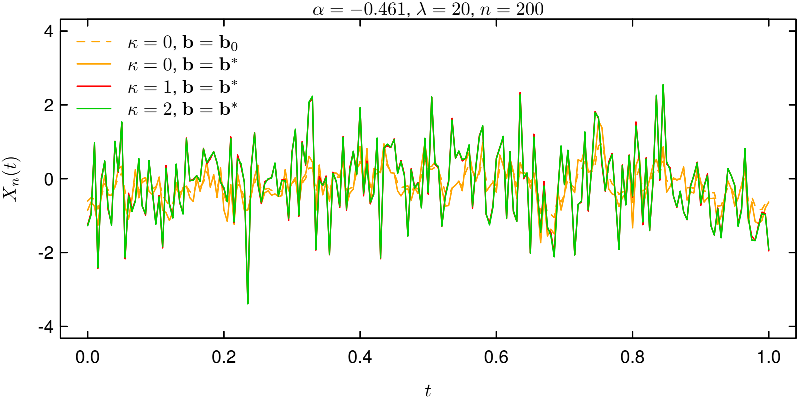

Using $g(x) = c_{\alpha,\lambda} x^{\alpha} e^{-\lambda x}$, with $c_{\alpha,\lambda}$ such that $\int_0^\infty g(x)^2 \mathrm{d}x = 1$.

Simulated trajectories

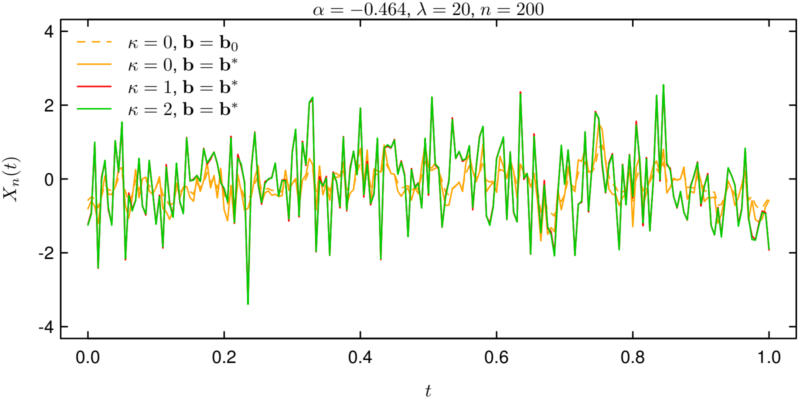

Using $g(x) = c_{\alpha,\lambda} x^{\alpha} e^{-\lambda x}$, with $c_{\alpha,\lambda}$ such that $\int_0^\infty g(x)^2 \mathrm{d}x = 1$.

Simulated trajectories

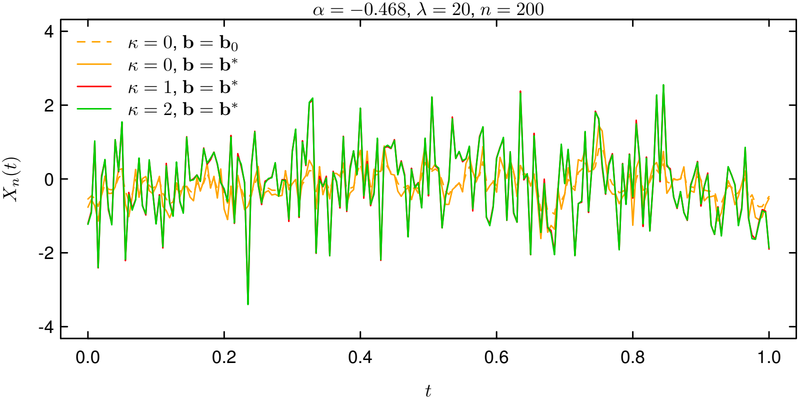

Using $g(x) = c_{\alpha,\lambda} x^{\alpha} e^{-\lambda x}$, with $c_{\alpha,\lambda}$ such that $\int_0^\infty g(x)^2 \mathrm{d}x = 1$.

Simulated trajectories

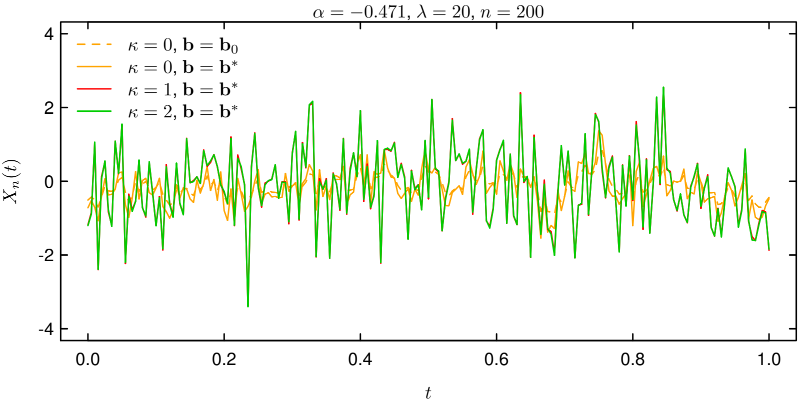

Using $g(x) = c_{\alpha,\lambda} x^{\alpha} e^{-\lambda x}$, with $c_{\alpha,\lambda}$ such that $\int_0^{\infty} g(x)^2 \mathrm{d}x = 1$.

Simulated trajectories

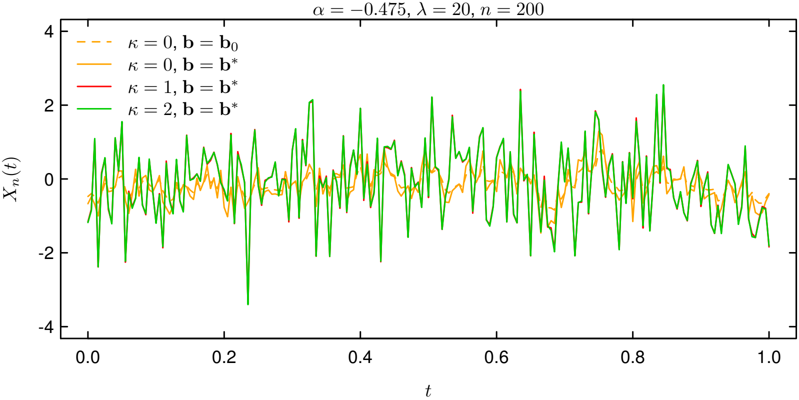

Using $g(x) = c_{\alpha,\lambda} x^{\alpha} e^{-\lambda x}$, with $c_{\alpha,\lambda}$ such that $\int_0^{\infty} g(x)^2 \mathrm{d}x = 1$.

Simulated trajectories

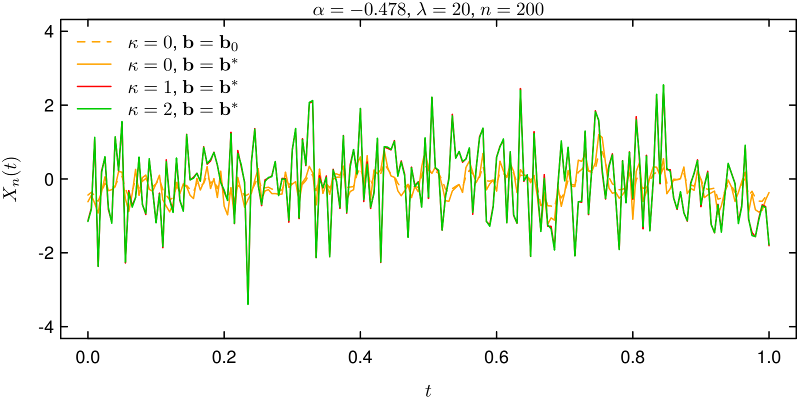

Using $g(x) = c_{\alpha,\lambda} x^{\alpha} e^{-\lambda x}$, with $c_{\alpha,\lambda}$ such that $\int_0^\infty g(x)^2 \mathrm{d}x = 1$.

Simulated trajectories

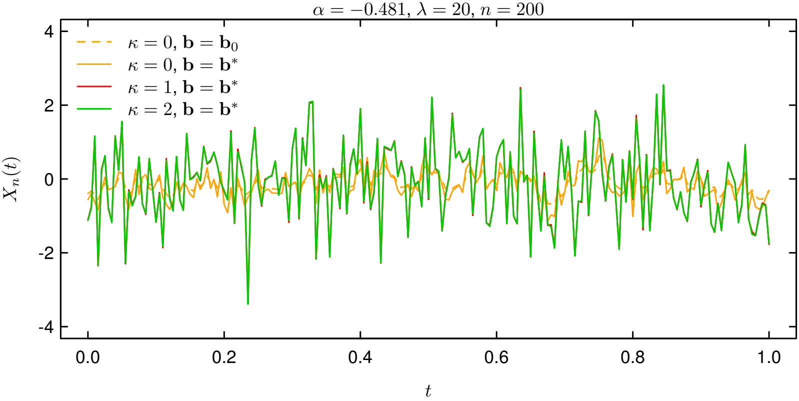

Using $g(x) = c_{\alpha,\lambda} x^{\alpha} e^{-\lambda x}$, with $c_{\alpha,\lambda}$ such that $\int_0^{\infty} g(x)^2 \mathrm{d}x = 1$.

Simulated trajectories

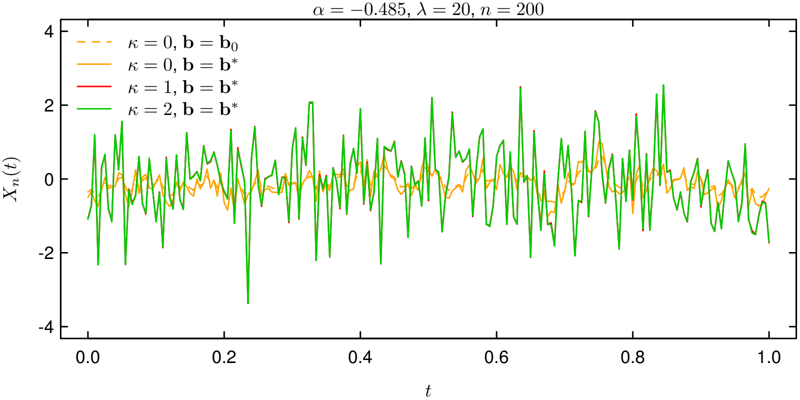

Using $g(x) = c_{\alpha,\lambda} x^{\alpha} e^{-\lambda x}$, with $c_{\alpha,\lambda}$ such that $\int_0^\infty g(x)^2 \mathrm{d}x = 1$.

Simulated trajectories

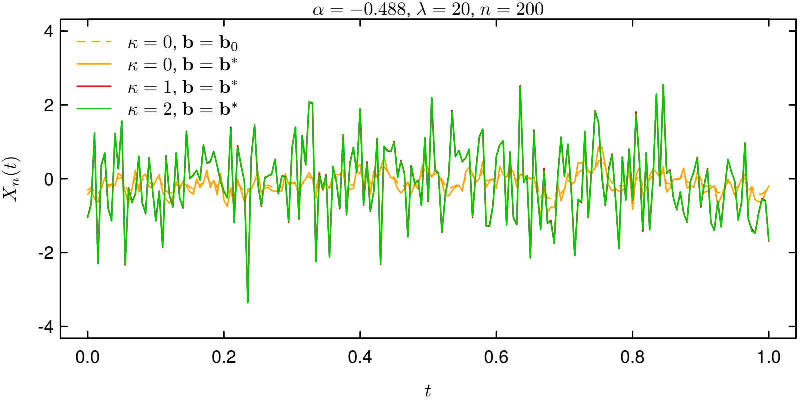

Using $g(x) = c_{\alpha,\lambda} x^{\alpha} e^{-\lambda x}$, with $c_{\alpha,\lambda}$ such that $\int_0^{\infty} g(x)^2 \mathrm{d}x = 1$.

Simulated trajectories

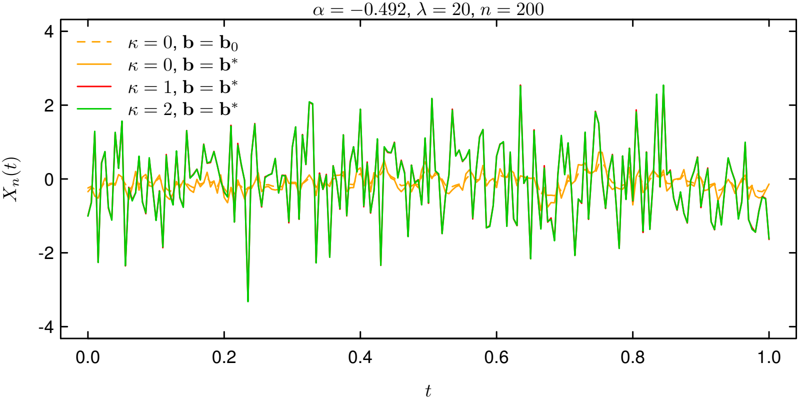

Using $g(x) = c_{\alpha,\lambda} x^{\alpha} e^{-\lambda x}$, with $c_{\alpha,\lambda}$ such that $\int_0^{\infty} g(x)^2 \mathrm{d}x = 1$.

Simulated trajectories

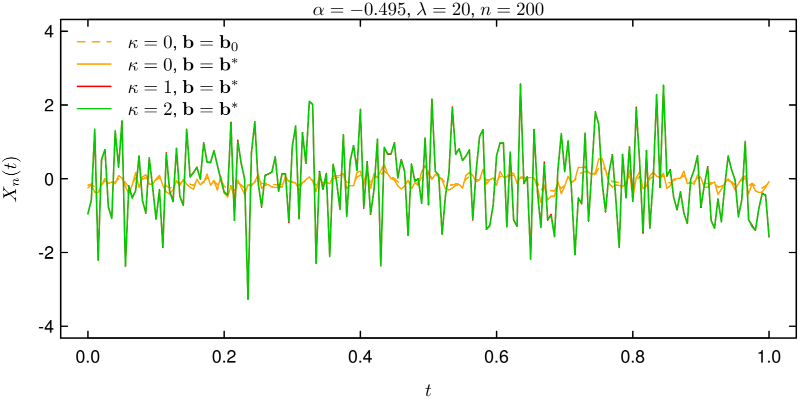

Using $g(x) = c_{\alpha,\lambda} x^{\alpha} e^{-\lambda x}$, with $c_{\alpha,\lambda}$ such that $\int_0^{\infty} g(x)^2 \mathrm{d}x = 1$.

Simulated trajectories

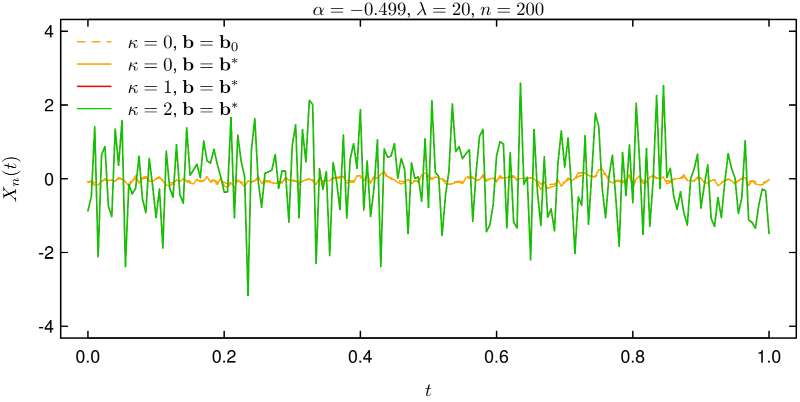

Using $g(x) = c_{\alpha,\lambda} x^{\alpha} e^{-\lambda x}$, with $c_{\alpha,\lambda}$ such that $\int_0^{\infty} g(x)^2 \mathrm{d}x = 1$.

Volatility-modulated moving average fields

In ongoing work with C. Heinrich and A. Veraart, we have adapted the hybrid scheme for the following class of random fields:

Definition

A 2-parameter volatility-modulated moving average ($\mathcal{VMMA}$) field $\{X(\boldsymbol{t})\}_{\boldsymbol{t}\in\mathbb{R}^2}$ is a covariance stationary random field defined by

$$X(\boldsymbol{t}) := \int_{\mathbb{R}^2} g(\boldsymbol{t}-\boldsymbol{s})\sigma(\boldsymbol{s})W(\mathrm{d}\boldsymbol{s}),$$

Volatility-modulated moving average fields

In ongoing work with C. Heinrich and A. Veraart, we have adapted the hybrid scheme for the following class of random fields:

Definition

A 2-parameter volatility-modulated moving average ($\mathcal{VMMA}$) field $\{X(\boldsymbol{t})\}_{\boldsymbol{t}\in\mathbb{R}^2}$ is a covariance stationary random field defined by

$$X(\boldsymbol{t}) := \int_{\mathbb{R}^2} g(\boldsymbol{t}-\boldsymbol{s})\sigma(\boldsymbol{s})W(\mathrm{d}\boldsymbol{s}),$$

where

- $g : \mathbb{R}^2 \to [0,\infty)$ is a square-integrable function,
- $\{\sigma(\boldsymbol{t})\}_{\boldsymbol{t}\in\mathbb{R}^2}$ is a covariance stationary random field with locally bounded realisations,
- W is a white noise on $\mathbb{R}^2$, independent of σ.

Class of kernel functions

Our hybrid scheme is applicable when the kernel function g has the form

$$g(\boldsymbol{x}) = \|A\boldsymbol{x}\|^{\alpha} L_g(\|A\boldsymbol{x}\|), \quad \boldsymbol{x} \in \mathbb{R}^2 \setminus \{\mathbf{0}\},$$

where $\alpha \in (-1,0)$, $A \in \mathrm{GL}(2)$, and $L_g : (0,\infty) \to [0,\infty)$ is slowly varying at 0.

Class of kernel functions

Our hybrid scheme is applicable when the kernel function g has the form

$$g(\boldsymbol{x}) = \|A\boldsymbol{x}\|^{\alpha} L_g(\|A\boldsymbol{x}\|), \quad \boldsymbol{x} \in \mathbb{R}^2 \setminus \{\boldsymbol{0}\},$$

where $\alpha \in (-1, 0)$, $A \in \mathrm{GL}(2)$, and $L_g : (0, \infty) \to [0, \infty)$ is slowly varying at 0.

The kernel function is isotropic if and only if A is orthogonal.

Class of kernel functions

Our hybrid scheme is applicable when the kernel function g has the form

$$g(\boldsymbol{x}) = \|A\boldsymbol{x}\|^{\alpha} L_g(\|A\boldsymbol{x}\|), \quad \boldsymbol{x} \in \mathbb{R}^2 \setminus \{\boldsymbol{0}\},$$

where $\alpha \in (-1,0)$, $A \in \mathrm{GL}(2)$, and $L_g : (0,\infty) \to [0,\infty)$ is slowly varying at 0.

The kernel function is isotropic if and only if A is orthogonal.

Example

Choosing $A = I_2$, $\alpha = \nu - 1$, $L(x) = x^{\frac{1-\nu}{2}} K_{\frac{1-\nu}{2}}(\lambda x)$, results in a Matérn (1960) covariance function

$$\mathbb{E}\big(X(\boldsymbol{0})X(\boldsymbol{h})\big) = \mathbb{E}\big(\sigma(\boldsymbol{0})^2\big) \frac{(\lambda\|\boldsymbol{h}\|)^{\nu}}{2^{\nu-1}\Gamma(\nu)} K_{\nu}(\lambda\|\boldsymbol{h}\|), \quad \boldsymbol{h} \in \mathbb{R}^2,$$

for $\nu \in (0,1)$ and $\lambda > 0$.

Hybrid scheme for $\mathcal{VMMA}$ fields

The hybrid scheme for $X\left(\frac{\boldsymbol{i}}{n}\right)$ is given (in the special case $A = I_2$) by

$$X\left(\frac{\boldsymbol{i}}{n}\right) \approx \sum_{\boldsymbol{k}\in K_\kappa} L_g\left(\frac{\boldsymbol{k}}{n}\right)\sigma\left(\frac{\boldsymbol{i}}{n} - \frac{\boldsymbol{k}}{n}\right) W^n_{\boldsymbol{i}-\boldsymbol{k},\boldsymbol{k}} + \sum_{\boldsymbol{k}\in \overline{K}_\kappa} g\left(\frac{\boldsymbol{b_k}}{n}\right)\sigma\left(\frac{\boldsymbol{i}}{n} - \frac{\boldsymbol{k}}{n}\right) W^n_{\boldsymbol{i}-\boldsymbol{k}},$$

Hybrid scheme for $\mathcal{VMMA}$ fields

The hybrid scheme for $X\left(\frac{\boldsymbol{i}}{n}\right)$ is given (in the special case $A = I_2$) by

$$X\left(\frac{\boldsymbol{i}}{n}\right) \approx \sum_{\boldsymbol{k}\in K_\kappa} L_g\left(\frac{\boldsymbol{k}}{n}\right)\sigma\left(\frac{\boldsymbol{i}}{n}-\frac{\boldsymbol{k}}{n}\right) W^n_{\boldsymbol{i}-\boldsymbol{k},\boldsymbol{k}} + \sum_{\boldsymbol{k}\in \overline{K}_\kappa} g\left(\frac{\boldsymbol{b_k}}{n}\right)\sigma\left(\frac{\boldsymbol{i}}{n}-\frac{\boldsymbol{k}}{n}\right) W^n_{\boldsymbol{i}-\boldsymbol{k}},$$

where

$$W^n_{\boldsymbol{i},\boldsymbol{j}} := \int_{\Delta_n \boldsymbol{i}} \|(\boldsymbol{i}+\boldsymbol{j})/n - \boldsymbol{s}\|^\alpha W(\mathrm{d}\boldsymbol{s}), \quad W^n_{\boldsymbol{i}} := \int_{\Delta_n \boldsymbol{i}} W(\mathrm{d}\boldsymbol{s}),$$

$$\Delta_n \boldsymbol{i} := \left(\frac{i_1-1/2}{n}, \frac{i_1+1/2}{n}\right] \times \left(\frac{i_2-1/2}{n}, \frac{i_2+1/2}{n}\right],$$

for $\boldsymbol{i},\boldsymbol{j} \in \mathbb{Z}^2$ and

Hybrid scheme for $\mathcal{VMMA}$ fields

The hybrid scheme for $X\left(\frac{\boldsymbol{i}}{n}\right)$ is given (in the special case $A = I_2$) by

$$X\left(\frac{\boldsymbol{i}}{n}\right) \approx \sum_{\boldsymbol{k}\in K_\kappa} L_g\left(\frac{\boldsymbol{k}}{n}\right)\sigma\left(\frac{\boldsymbol{i}}{n}-\frac{\boldsymbol{k}}{n}\right) W^n_{\boldsymbol{i}-\boldsymbol{k},\boldsymbol{k}} + \sum_{\boldsymbol{k}\in \overline{K}_\kappa} g\left(\frac{\boldsymbol{b_k}}{n}\right)\sigma\left(\frac{\boldsymbol{i}}{n}-\frac{\boldsymbol{k}}{n}\right) W^n_{\boldsymbol{i}-\boldsymbol{k}},$$

where

$$W^n_{\boldsymbol{i},\boldsymbol{j}} := \int_{\Delta_n \boldsymbol{i}} \|(\boldsymbol{i}+\boldsymbol{j})/n - \boldsymbol{s}\|^\alpha W(\mathrm{d}\boldsymbol{s}), \quad W^n_{\boldsymbol{i}} := \int_{\Delta_n \boldsymbol{i}} W(\mathrm{d}\boldsymbol{s}),$$

$$\Delta_n \boldsymbol{i} := \left(\frac{i_1-1/2}{n}, \frac{i_1+1/2}{n}\right] \times \left(\frac{i_2-1/2}{n}, \frac{i_2+1/2}{n}\right],$$

for $\boldsymbol{i},\boldsymbol{j} \in \mathbb{Z}^2$ and

$$K_\kappa := \{-\kappa,\ldots,\kappa\}^2, \quad \overline{K}_\kappa := \{-N_n,\ldots,N_n\} \setminus K_\kappa,$$

with $N_n > \kappa \geqslant 0$ and $\boldsymbol{b_k} \in (k_1 - \frac{1}{2}, k_1 + \frac{1}{2}] \times (k_2 - \frac{1}{2}, k_2 + \frac{1}{2}]$ for $\boldsymbol{k} \in \mathbb{Z}^2$.

Simulated realisations

$\alpha = -0.1, \quad A = I_2$

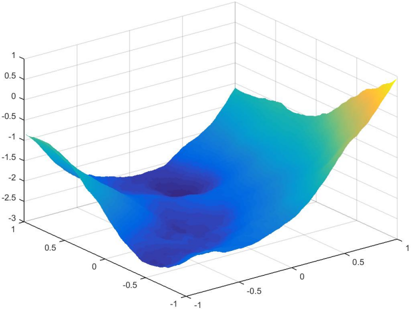

$\alpha = -0.3, \quad A = I_2$

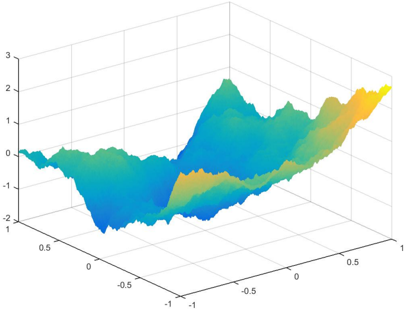

$$g(\boldsymbol{x}) = \|A\boldsymbol{x}\|^{\alpha} e^{-\|A\boldsymbol{x}\|}, \quad \sigma(\boldsymbol{s}) = 1.$$

Simulated realisations

$$\alpha = -0.8, \quad A = I_2$$

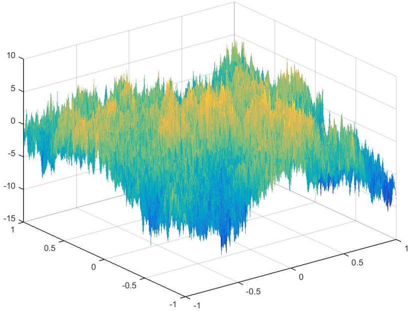

$$\alpha = -0.5, \quad A = \frac{1}{3}\begin{bmatrix} 2 & 1 \\ 1 & 1 \end{bmatrix}$$

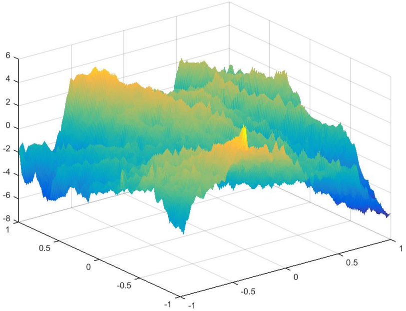

$$g(\boldsymbol{x}) = \|A\boldsymbol{x}\|^{\alpha} e^{-\|A\boldsymbol{x}\|}, \quad \sigma(\boldsymbol{s}) = 1.$$

References

- O. E. Barndorff-Nielsen and J. Schmiegel (2009): Brownian semistationary processes and volatility/intermittency. In *Advanced financial modelling,* Volume 8 of *Radon Ser. Comput. Appl. Math.*, pp. 1–25. Berlin: Walter de Gruyter.
- M. Bennedsen, A. Lunde, and M. S. Pakkanen (2015): Hybrid scheme for Brownian semistationary processes. *Preprint,* `http://arxiv.org/abs/1507.03004`.
- B. Matérn (1960): Spatial variation: Stochastic models and their applications to some problems in forest surveys and other sampling investigations. *Meddelanden från Statens Skogsforskninginstitut, Band 49, Nr. 5, Stockholm.*
- A. T. A. Wood and G. Chan (1994): Simulation of stationary Gaussian processes in $[0,1]^d$. *J. Comput. Graph. Statist.* **3**(4), 409–432.

Slow variation at zero

Definition

A function $L\colon (0,1] \to [0,\infty)$ is slowly varying at 0 if for any $t > 0$,

$$\lim_{x\to 0+} \frac{L(tx)}{L(x)} = 1.$$

The intuition is that such a slowly varying function varies "less" than any power function "near" zero. Examples:

- If $\lim_{x\to 0+} L(x) \in (0,\infty)$ exists, then L is slowly varying.
- The function $L(x) = -\log x$ is slowly varying.

Back to assumptions

Implementation of the $\mathcal{BSS}$ hybrid scheme

Outline of implementation

Generating $X_n\left(\frac{i}{n}\right)$ for $i = 0, 1, \ldots, \lfloor nT \rfloor$ involves:

1. sampling $\lfloor nT \rfloor + N_n$ iid observations from a $\kappa + 1$ dimensional Gaussian distribution,
2. generating a discretisation of σ using some appropriate scheme,
3. computing the observations by summation and discrete convolution (using FFT).

- Glossing over the simulation of σ, the computational complexity of this procedure is $\mathcal{O}(N_n \log N_n) = \mathcal{O}(n^{1+\gamma} \log n)$.
- The computational complexity of an exact simulation in the Gaussian case would be $\mathcal{O}(n^3)$ (using Cholesky decomp.).

◂ Back to hybrid scheme